

Preparation of Eco-Friendly Nanocatalyst Calcium Oxide (CaO) for Oily Wastewater Treatment by Advanced Oxidation Process

¹Eman H. Khader, ¹Thamer J. Mohammed, ¹Talib M. Albayati*, ²Sohrab Zendehboudi

¹Department of Chemical Engineering, University of Technology – Iraq, Iraq

²Department of Process Engineering, Memorial University, St. John's, Canada

ARTICLE INFO

Article history:

Received: August, 13, 2024

Accepted: December, 17, 2024

Available online: March, 10, 2025

Keywords:

Degradation efficiency,
Eco-friendly photocatalyst,
Green nanocatalyst,
Oily wastewater,
Photocatalytic

*Corresponding Author:

Talib M. Albayati

talib.m.naieff@uotechnology.edu.iq

ABSTRACT

In the present work, a novel eco-friendly nanocatalyst (NC) calcium oxide (CaO) is synthesized from the waste of tomato plants by physical method for the degradation of oil in oily wastewater by photocatalytic technology as a sophisticated oxidation process. The characterization of NC prepared is described by dynamic light scattering (DLS), Brunauer-Emmett-Teller (BET) analysis, Fourier transform infrared spectroscopy (FTIR), field emission scanning electron microscopy (FE-SEM), X-ray powder diffraction (XRD), and energy-dispersive X-ray (EDX) spectroscopy, which illustrated that the NC prepared possessed a nanoscale size and a cubic crystal structure. The activity of NC in the photodegradation process is evaluated using oil concentration (100–500 ppm), amount of NC (0.1–1) g/L, and pH (4–12) at a specific aeration rate of 1 L/min and time irradiation of 30–180 min and under UV light. The findings showed that the degradation efficiency of oil increased with an increased amount of NC, time, and pH while decreasing with increased oil concentration. The maximum degradation of oil reached 83.0% at optimum conditions (oil concentration = 100 ppm, amount of NC = 0.6 g/L, pH = 7, time of irradiation = 120 min, and temperature = 23 °C). This work illustrates that the novel NC can be employed as an environmentally friendly and economical photocatalyst and might be improved in its characteristics and performance by thermal technique (calcination) to enhance the reduction of oil from oily wastewater.

<https://doi.org/10.53293/jasn.2024.7482.1312>, Department of Applied Sciences, University of Technology - Iraq.

© 2024 The Author(s). This is an open access article under the CC BY license (<http://creativecommons.org/licenses/by/4.0/>).

1. Introduction

The rapid growth in population and industrial development has resulted in a significant rise in the production of oily wastewater. This wastewater is generated at an alarming rate from activities across various industries, including food and beverage production, petrochemicals, petroleum refineries, and the oil and gas industries, etc. This wastewater contains numerous toxic contaminants, posing serious risks to human health and the environment including total suspended solids, biochemical oxygen demand, chemical oxygen demand, total petroleum hydrocarbon, heavy metals, oil and grease, phenolic compounds, and aromatic organic compounds, etc. Additionally, oil in the wastewater can degrade into other harmful chemicals, further aggravating environmental

contamination and negatively impacting human health and aquatic organisms [1–3]. Therefore, oily wastewater is considered a source of water pollution, often containing oil and grease concentrations between 100 and 5000 ppm, or even higher, depending on the type of crude oil involved [4]. According to the environmental guidelines, the allowable discharge level for oil and grease is between 10 and 15 ppm. As a result, the oily wastewater must be treated [5]. Various techniques were employed for treating oily wastewater and the reduction of its effect on the environment including physical, chemical, and biological processes [6, 7]. However, physical methods for treating oily wastewater tend to have low pollutant removal efficiency, require substantial installation space, consume high energy for coagulant dispersion, and are time-intensive for separating oil through gravity [8–10]. Chemical techniques are not environmentally friendly, consume hazardous substances, have expensive chemical costs, and produce secondary contaminants [11–13]. Biological treatment methods are highly sensitive to changes in temperature, feeding composition, oxygen levels, and other environmental factors, all of which can significantly impact their effectiveness. Furthermore, using these techniques cannot effectively degrade the compounds of oil, which include asphaltenes, aromatics, resins, and saturated compounds, as well as cannot eliminate toxic compounds and microorganisms with efficiency [14]. Thus, the application of advanced treatment methods is essential, as they are considered sustainable, cost-effective, eco-friendly, and effective methods for eliminating contaminants from oily wastewater [15, 16]. In this regard, advanced oxidation methods (photolysis, Fenton, photo-Fenton, and photocatalytic) are effective technologies for degrading organic pollutants, including grease and dispersed and dissolved oil in oily wastewater [17]. Especially, the photocatalytic process emerges as an excellent method for the reduction of contaminants in wastewater because of its nontoxicity, low cost, and mineralization effectiveness. [18]. Photocatalysis utilizes light (UV/sunlight) and a catalyst to trigger chemical reactions (oxidation and reduction reaction) to generate hydroxyl and superoxide radicals; These radicals are generated when a photocatalyst is exposed to light, exciting electrons from the valance band to the conduction band, leaving behind holes in the catalyst. Hydroxyl radicals are formed when holes in the valance band oxidize water or hydroxide ions, while superoxide radicals are formed when electrons in the conduction band reduce oxygen. These radicals are highly reactive with pollutants and contribute to degrading them into CO₂ and H₂O (compounds less harmless) [19]. Various metal oxide nanoparticles (NPs) serve as highly effective photocatalysts because of their relatively low toxicity and ease of oxidation into hydroxides or oxides [20]. Examples include TiO₂, ZnO, Fe₂O₄, WO₃, CuO, Cu₂O, SnO₂, CaO, and CeO₂. These metal oxides are available in numerous morphologies, such as nanoparticles, nanospheres, nanofibers, nanotubes, nanoribbons, and nanosheets [21–23].

Different physical, chemical, and biological methods can be effectively used to prepare nanocatalysts. Physical and chemical methods include microemulsion, aerosol technologies, microwave, mechanical milling, lithography, laser ablation, sol-gel, sonochemical, ultrasonic spark discharge, ion sputtering, photochemical reduction, and template synthesis. Bacteria, fungi, and algae are typically used in biological synthesis techniques [24].

Synthesizing nanoparticles using plant extracts as photocatalysts is a highly advantageous method, offering low energy requirements, scalability, biocompatibility, rapid synthesis, sustainable stability of the resulting NPs and less expensive, enabling the creation of NPs in various sizes and shapes [26, 25]. Thus, due to their relative abundance and inexpensive cost, green photocatalysts are a possible substitute [27]. Agricultural waste, being abundant and naturally occurring, with numerous surface functional groups, can act as an economical alternative to expensive semiconductor photocatalysts [28]. Kaur *et al.* [29] prepared nanocomposites from the flower extract of *Hibiscus rosa sinensis* by the hydrothermal method for the removal of dye and heavy metals from wastewater. Hasan *et al.* [30] synthesized nanocomposite from the aqueous leaf extract of *Laurus nobilis* for oily wastewater treatment. De Menezes *et al.* [31] synthesized CaO NPs from golden linseed (*Linum usitatissimum* L.) extract by the biosynthesis method for the removal of yellow tartrazine dye.

The major objective of this research is to synthesize an eco-friendly nanocatalyst (NC) from the waste of a tomato plant for the first time for the degradation of oil in oily wastewater. The characterization of prepared NC was determined by dynamic light scattering, Fourier-transformed infrared spectra, Brunauer-Emmett-Teller surface area, X-ray powder diffraction, field emission scanning electron microscopy, and energy dispersive X-ray spectroscopy. Furthermore, the impact of several variables on the photocatalyst degradation of oil was tested, including the nanocatalysts' dosage, irradiation time, pH, and oil concentration.

2. Materials and Methods

2.1. Materials

The waste of tomato plants was provided by groves. High-purity sodium dodecyl sulfate (SDS), HCl, and NaOH were supplied from HD Agro Chemicals, India. Heavy oil was provided by South Refineries Company in Iraq.

2.2. Preparation of Nanocatalyst

To prepare the nanocatalyst, the waste from tomato plants, specifically the sepals (outer parts of the flower), was thoroughly rinsed multiple times with distilled water to erase any organic debris, soil, and dust from the surface. It was then dried in a furnace at 70 °C for 2 hours. Finally, the material was milled using a grinding device (MM8-300, NIMA, Japan). The dried NC was then milled and passed through a sieve analysis instrument (As 200 DIGIT CA, RETSCH, Japan) to obtain a fine NC powder with a particle size of less than 75 µm. Fig. 1 illustrates the steps of preparation for NC.



Figure 1: Steps of preparation for the nanocrystals.

2.3. Synthesis of Oily Wastewater

To synthesize oily wastewater different heavy oil concentrations were mixed with distilled water in the existence of an emulsifier (SDS) at a weight ratio of 1 for each 10 of heavy oil using a homogenizer instrument (FSH -2A, LAWSON, China) at a speed of 18,000 rpm for 15 min continuously. The concentration of oil in oily wastewater was determined by an oil content analyzer (Hcy-20, Zhejiang Top Cloud-Agri Technology Co., Ltd., China).

2.4. Characterization of Nanocatalyst

Fourier-transform infrared (FTIR) spectroscopy (FTIR-7600, Lambda, USA) was utilized to identify the functional groups present in the NC. The crystal structures of the NC were analyzed using X-ray powder diffraction (TD-3700, Tongda, China). To examine the morphology and particle distribution, field-emission scanning electron microscopy (FE-SEM) (JCS5592, Shimadzu, Japan) was employed. The chemical composition was determined with FE-SEM coupled with energy-dispersive X-ray (EDX) spectroscopy. The dynamic light scattering (DLS) technique (90 plus, Brookhaven Instruments Corp., USA) was used to measure the average particle size of the NC. Additionally, the evaluation of the surface area using the Brunauer–Emmett–Teller (BET) method (BELSORP-MaxII, India).

2.5. The Photodegradation Method Experimental Setup

The photocatalysis method was executed in the reactor of 1 L type cylindrical, as shown in Fig. 2. The variables studied in the photocatalysis degradation experiments included pH (4–12), amount of NC (0.1–1) g/L, irradiation time (30–180 min), and oil concentration (100–500 ppm). Different doses of NC were blended with oily wastewater (0.5 L) and mixed at a speed of 300 rpm for 30 min in the dark to assert the adsorption-desorption

equilibrium. Later, this mixture was irradiated by UV (5-lamp) light to degrade the oil in oily wastewater and pump air with an aeration rate of 1 L/min. Samples of the treated oily wastewater were collected, and the oil content was evaluated after a period of time. The oil degradation efficiency was determined by Eq. (1).

$$\text{Oil degradation \%} = \left(1 - \frac{C}{C_0}\right) \times 100 \quad (1)$$

where C_0 refers to the initial concentration of oil and C represents overtime concentration of oil [32].

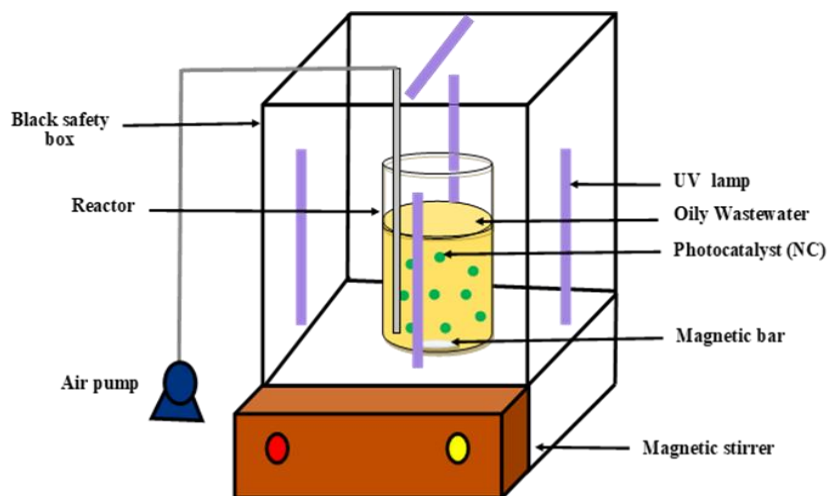


Figure 2: Experimental setup of photocatalytic process.

3. Results and Discussion

3.1. Characterization of NC

The characterization of a nanocatalyst involves studying its physical and chemical properties to understand its effectiveness in the photocatalytic process. It includes the following:

3.1.1. The Mean Particle Size of NC

The distribution of NC particle size was determined via the DLS method, revealing an average particle size of 135.7 nm, as seen in Fig. 3. This value indicates that the prepared NC is a nanoparticle with a small size.

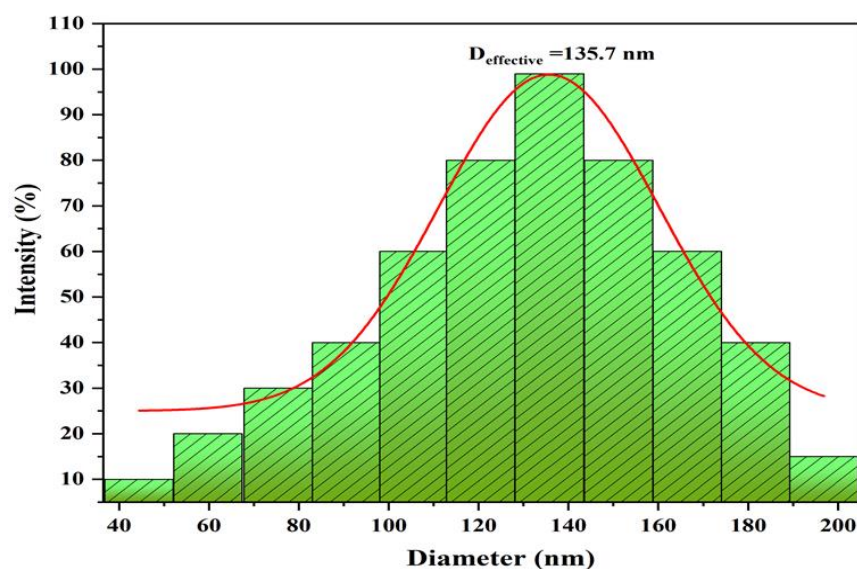


Figure 3: Particle size distribution of nanocrystals.

3.1.2 XRD Analysis

The details that describe the crystal structure of the NC are displayed in Fig. 4, which confirms that the significant diffraction peaks of NC are found at $2\theta = 14.7, 24.2, 26.5, 28.1, 29.9, 34.9, 40.4, 43.2, 57.3$ and 66.2 , which are associated with the Miller indices (001), (012), (111), (202), (104), (200), (114), (102), (220), and (311), respectively. This analysis shows that the sample of NC contains a significant amount of cubic phase (CaO) (JCPDS No. 00-017-0912) as the major phase and rhombohedral calcite phase (CaCO₃) as the minor phase. The peak at $2\theta = 28.1$ indicates the existence of CaO in the NC structure.

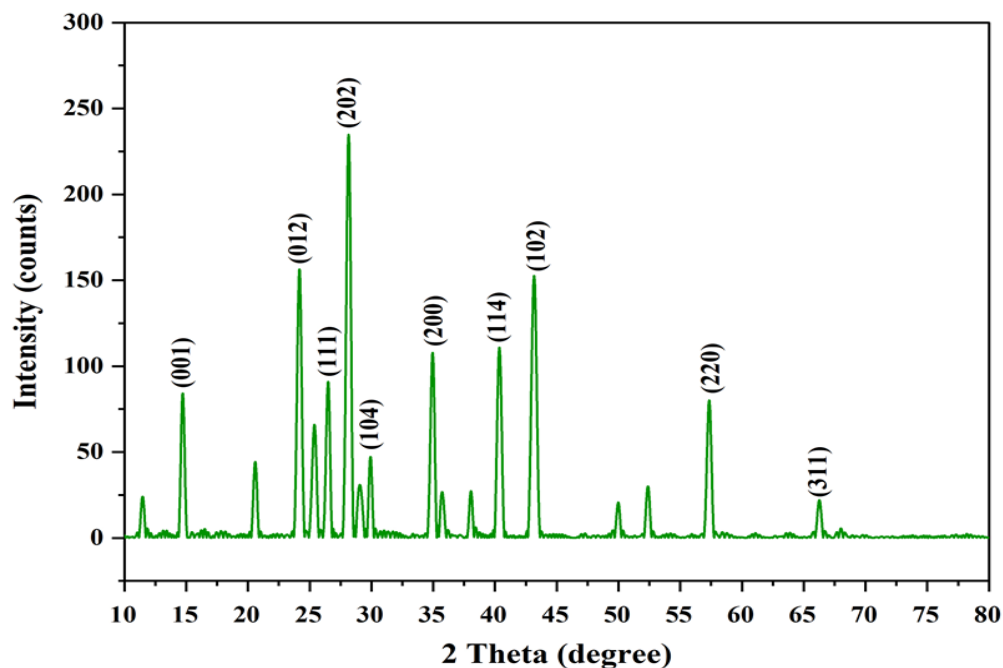


Figure 4: XRD pattern of the nanocrystals.

3.1.3 FTIR Analysis

Fig. 5 describes the FTIR spectra of NC. It is noted that the peak located at 3395 cm^{-1} is associated with the stretching vibration band of acidic OH groups. A peak at 2924 cm^{-1} corresponds to C-H stretch bonds. The band at 1643 cm^{-1} belongs to the carboxyl group (C=O) stretching vibration [33]. A bond at 1416 cm^{-1} is due to ionic carboxylic groups ($-\text{COO}-$) symmetric stretching vibration. A peak at 1319 cm^{-1} denotes the C-N stretch, which is the characteristic peak of polysaccharides, while the influence of the C-O group appears at peaks 1238 cm^{-1} and 1103 cm^{-1} [34, 35]. The bond at 606 cm^{-1} indicates the C-H group. The peak at 459 cm^{-1} is assigned to the Ca-O bond [36]. Table 1 illustrates the details of function group by FTIR.

Table 1: illustrated the details of function group by FTIR

Wave number (cm^{-1})	Vibration type	Bond assignment	Ref.
3395	Stretching	O-H	[33]
2924	Stretching	C-H	[33]
1643	Stretching	C=O	[33]
1416	Symmetric stretching	C=O	[34]
1319	Stretching	C-N	[34]
1238	Stretching	C-O	[34]
1103	Stretching	C-O	[35]
606	Rocking	C-H	[35]
459	Stretching	Ca-O	[36]

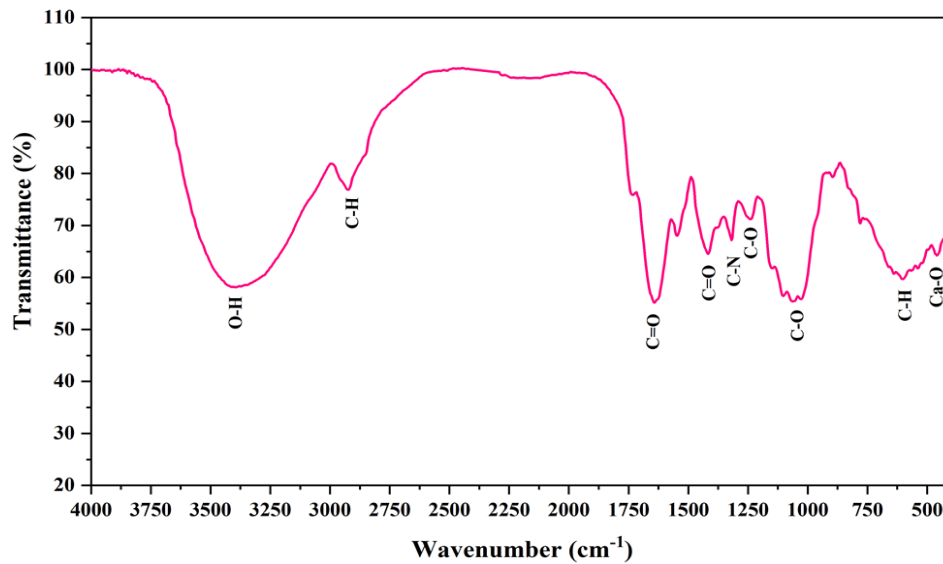


Figure 5: FTIR spectrum of nanocrystals.

3.1.3 EDX and FE-SEM Analyses

The EDX analysis showed the elemental compositions of the NC, as depicted in the left side of Fig. 6. From Fig. 6, it is observed the amount of Ca, O, C, Al, Mg, Na, Si, and Cl was 35.1 wt. %, 27.2 wt. %, 21.6 wt. %, 8.4 wt. %, 3.6 wt. %, 1.7 wt. %, 1.5 wt. %, and 0.9 wt. %. The right of Fig. 6. represents the 50 μm magnification of the CaO sample that conducted analyses of the EDX. The analysis results of the NC indicate that elements Ca, O, and C are present in the highest percentages.

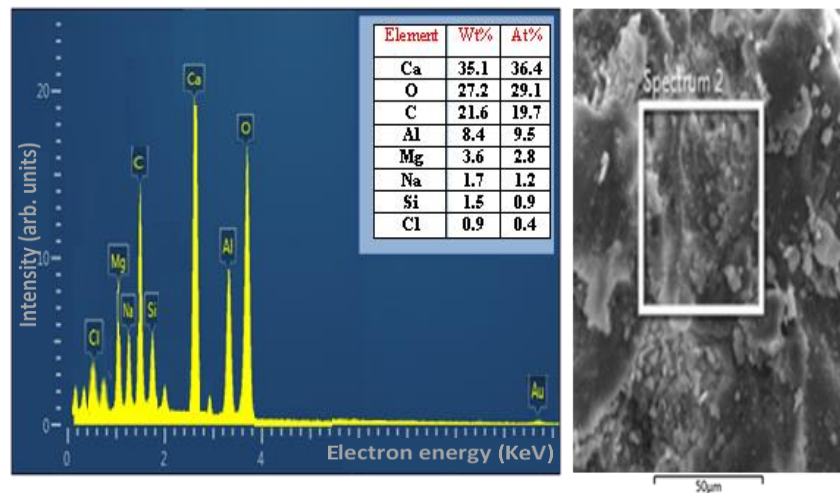


Figure 6: EDX spectroscopy of the nanocrystals.

The micrographs of NC by FE-SEM are depicted in Fig. 7. The distribution of NC particle size showed inhomogeneities, with particle sizes ranging between 48 and 194 nm (Fig. 7 (c and d)). The NC average particle size is less than 136 nm. Furthermore, the NC powders exhibit various shapes due to irregular grinding (Fig. 7 (b)). The surface of the NC appears smooth, with a small porous structure (Fig. 7 (a)). FE-SEM shows some agglomerations due to inhomogeneity in particle size distribution, where the smaller particles may become trapped between larger ones, or due to inter-particle forces (van der Waals forces), these forces can cause small particles to adhere together, leading to agglomeration, especially in fine powders.

The surface properties of the NC were measured, resulting in a pore volume of approximately 0.4535 cm³/g, a pore size of 83.292 nm, and a surface area of 19.73 m²/g.

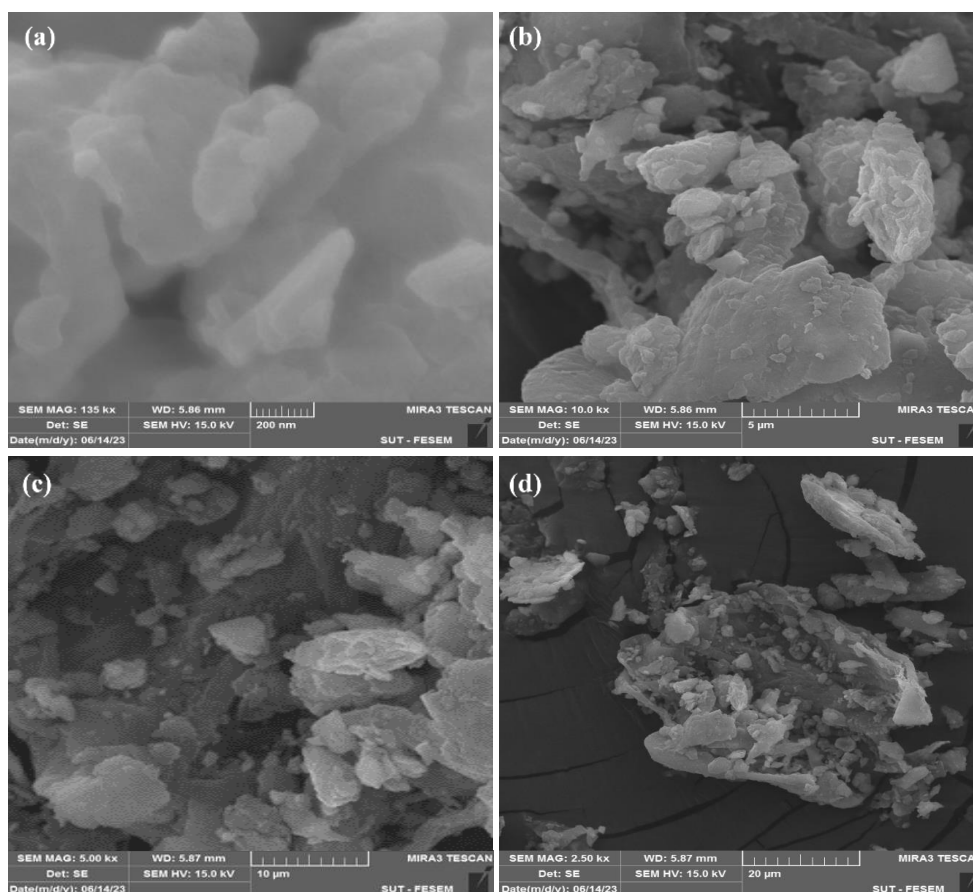


Figure 7: FESEM spectroscopy of NC with different magnifications (a) 135KX, (b) 10KX, (c) 5KX, and (d) 2.5KX.

3.2 Performance of Photocatalytic for Degradation Oil

The performance of a photocatalytic process for degradation oil is often assessed based on the factors that influence it, including as follows:

3.2.1 Impact of NC Dose

The impact of the NC amount dose on the degradation of oil in oily wastewater is demonstrated in Fig. 8. The tests were carried out at NC doses of 0.1–1 g/L, a pH of 7, oil concentration of 100 ppm, and aeration rate of 1L/min under UV irradiation for 90 min. The findings revealed that the degradation rate of oil increased with the rising doses of NC added; however, the degradation rate subsequently decreased when the amount of NC was increased further. The removal efficiency increased from 31.0% to 73.0% when raising the amount of NC from 0.1 to 0.6 g/L. This is attributed to an increase in the number of active sites existing for light absorption and the formation of radicals, which occurs up to a certain limit with the addition of NC at 0.6 g/L. Additionally, the enhanced photoreaction rate is because of the large surface area of the NC, which facilitates both degradation and adsorption processes, which contributed to an increase in the production of hydroxyl and superoxide radicals. Hydroxyl radicals are highly reactive and non-selective, capable of oxidizing most organic pollutants (e.g., oil) to CO_2 and H_2O . In contrast, the superoxide radicals can degrade oil to CO_2 and H_2O and contribute to the formation of additional hydroxyl radicals, thereby improving the degradation efficiency of oil [37, 38].

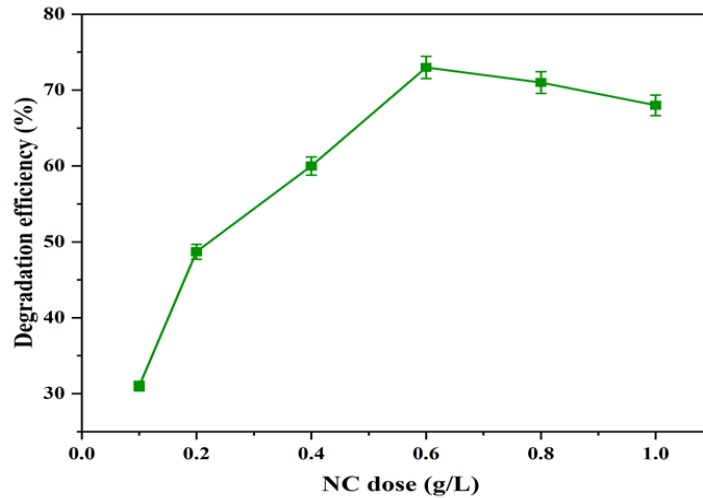


Figure 8: Oil degradation efficiency at various amounts of nanocrystals.

In contrast, the degradation efficiency declined to 71.0% and 68.0% with a further increase in the amount of NC from 0.8 to 1 g/L. This is due to the agglomeration of NC in high amounts and the increase in the interaction between particles, which causes a loss in its surface area, thus making its surfaces unavailable for photon absorption due to the interception of light [39, 40]. Also, the presence of NC in high amounts can cover the active sites (specific locations where the photocatalytic reaction occurs) and cause water turbidity, hindering light penetration into the reaction medium; consequently, degradation efficiency and NC photocatalytic ability are reduced after the increase of NC more than 0.6 g/L. These findings agree with the findings of the research conducted by Khader *et al.* [41].

3.2.2 Impact of pH

To evaluate the impact of oily wastewater pH on the activity of oil photodegradation, the experiments were conducted under operating conditions with pH values ranging from 4 to 12, an NC amount of 0.6 g/L, an oil concentration of 100 ppm, aeration rate of 1 L/min, and exposure irradiation time of 90 min, as illustrated in Fig. 9. The data showed that the degradation efficiency of oil rose from 69.3% to 81.5% as the pH value rose from 4 to 12. This can be explained by the increased concentration of hydroxyl ions (OH^-) at higher pH levels, which can significantly enhance the efficiency of photocatalytic reactions. This increase in hydroxyl ions leads to more production of hydroxyl radicals, resulting in more effective oil degradation [42, 43].

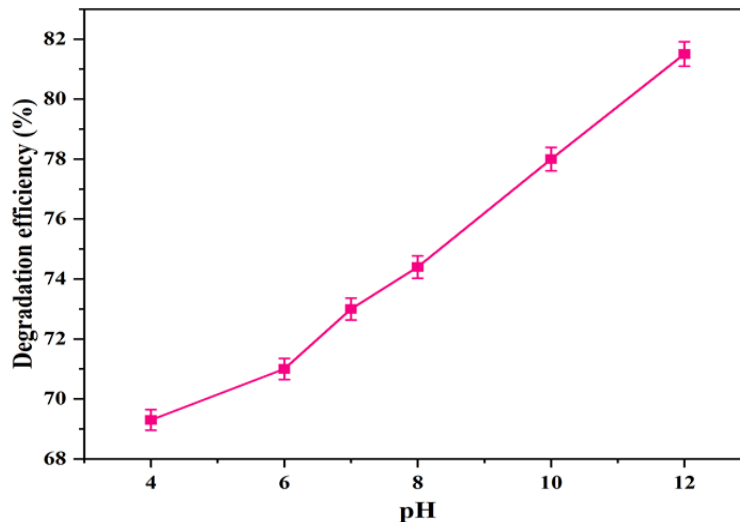


Figure 9: Oil degradation efficiency at various pH values of oily wastewater.

3.2.3 Impact of Irradiation Time

The irradiation time impact on the removal efficiency of oil is depicted in Fig. 10a. The photocatalytic experiments were carried out employing 100 ppm of oil concentration, a pH of 7, an NC dose of 0.6 g/L, and an irradiation time of 30–180 min with an aeration of 1 L/min. The findings observed that the oil removal efficiency increased from 52.5% to 83.0% with an increase in irradiation time from 30 to 120 min, reaching equilibrium after 120 min. These results are due to the increased interaction between oil and the photocatalyst surface, which increased the photodegradability of the photocatalyst and improved the degradation efficiency of oil as the irradiation time increased [44]. The degradation efficiency remained approximately constant with a further increase in irradiation time from 120 to 180 min because of the active site saturation of the NC surface, which caused this equilibrium [45]. Similar results are obtained by Khader *et al* [46].

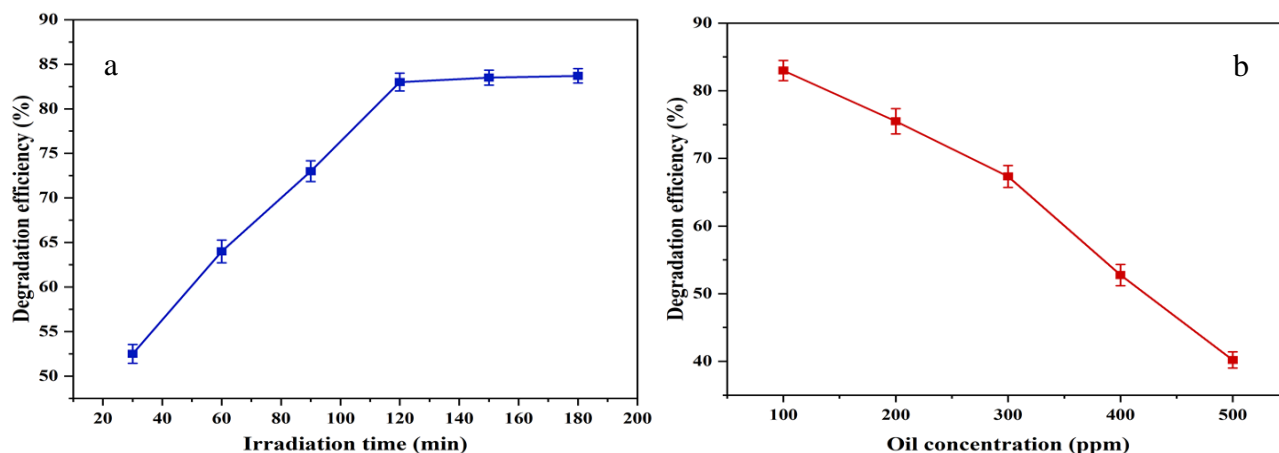


Figure 10: a) Oil degradation efficiency under various irradiation times. b) Oil degradation efficiency at various oil concentrations.

3.2.4 Impact of Oil Concentrations

Fig. 10b demonstrates the influence of oil concentrations on oil removal efficiency. The tests were performed at varying oil concentrations between 100 and 500 ppm, amount of NC (0.6 g/L), pH of the wastewater is 7 with an irradiation time of 120 min and an aeration rate of 1 L/min. The results revealed that the oil degradation efficiency decreased from 83.0% to 40.2% as the oil concentration increased from 100 to 500 ppm. This is due to the solution becoming darker with the rise in oil concentration, where the oil itself will absorb light instead of the NC, which will decline the activity of oil photodegradation. Additionally, high oil concentrations can block the active sites of the nanocatalyst, leading to a decrease in the formation of hydroxyl radicals ($\text{OH}\cdot$). An increase in oil concentration can lower light absorption by reducing the number of photons that reach the photocatalyst's surface, which diminishes the production of electron-hole pairs and, consequently, decreases the efficiency of oil degradation. [47, 48].

3.3. Comparison With The Works of Literature

Table 2 compares the performance of the NC (CaO) photocatalyst developed in this study with previous research on photocatalysis using various green photocatalysts synthesized from plant extracts and their effectiveness in pollutant removal from many sources of wastewater. It is evident from Table 2 that researchers have not utilized any green nanocatalysts, particularly those derived from waste tomato plants, for the photocatalytic degradation of oil in wastewater. This highlights that the novel NC (CaO) can serve as an eco-friendly photocatalyst for the removal of oil from oily wastewater.

Table 2: Comparative study between different types of green photocatalysts synthesized from plants for degradation of pollutants in wastewater.

Material of synthesis catalyst	Method	Application	Pollutant	Degradation %	Ref.
Moringa oleifera seed (Ag)	Biosynthesis	Toxic pollutants in wastewater	Methylene blue	81	[49]
			Orange-red dye	82	
			4-nitrophenol	75	
			Pb	80	
Moringa oleifera leaf (ZnO)	Biosynthesis	Petroleum refinery wastewater	Phenol	51	[50]
			o-cresol	52	
			Toluene	88	
			Xylene	93	
Cymbopogon citratus (ZnO)		Palm oil mill effluent	Turbidity	68.03	[51]
			Color	48.11	
			COD	75.40	
Golden linseed (CaO)	Biosynthesis	Wastewater	Tartrazine dye	76.20	[31]
Laurus nobilis leaf	Biosynthesis	Oily wastewater	Rose Bengal	96.8	[30]
			Methylene blue	90.1	
			Toluidine blue	93.8	
			Heavy metals	99–100	
			Total petroleum Hydrocarbons	98.0	
			Total suspended solids	91.8	
Jatropha curcas leaf (TiO ₂)	Chemically synthesis	Tannery wastewater	COD	82.26	[52]
			Cr	76.48	
Garlic bulbs plant extract	Chemically synthesis	Wastewater	Methylene blue	94	[53]
Seriphidium oliverianum leaf (CuO)	Bio-mechanochemical ly synthesis	Wastewater	Methyl green	65.23	[54]
			Methyl orange	65.07	
Crataegus pontica C.Koch leaves (CaO)	Chemically synthesis	Wastewater	Methylene blue	98.99	[55]
Tomato sepals (CaO)	Physical synthesis	Oily wastewater	Oil	83	This work

4. Conclusions

This study synthesized CaO nanocatalyst from the waste of a tomato plant for the first time and employed it for the treatment of oily wastewater through the photodegradation of oil. The analyses (DLS, XRD, FTIR, EDX, BET, and FE-SEM) that described NC characterization proved an excellent crystallized structure and nanosized for photocatalyst. This study demonstrated that the degradation efficiency of oil improved with increases in NC dose, pH, and irradiation time, while it decreased with higher oil concentrations. The results confirmed that the activity of 0.6 g/L of NC for degradation oil was 83.0% (residual = 17 ppm) under UV irradiation for 120 min with a pH of 7, an aeration rate of 1 L/min, and an oil concentration of 100 ppm. Therefore, it is recommended to improve the activity of NC by thermal technique to achieve excellent degradation of oil to meet the requirement of the World Health Organization's (WHO) of 5 ppm for oil content in wastewater discharge into the environment. In addition, it is recommended to use other plant waste for the preparation of photocatalysts as a result of their availability and being eco-friendly materials.

Acknowledgement

The authors are grateful to the Department of Chemical Engineering at the University of Technology-Iraq, the Department of Civil Engineering, Memorial University, St. John's, NL A1B 3X5, Canada, and the Department of Process Engineering, Memorial University, St. John's, NL A1B 3X5, Canada.

Conflict of Interest

The authors declare that they have no conflict of interest.

References

- [1] Y.-Z. Song, X. Kong, X. Yin, Y. Zhang, C. C. Sun, J. J. Yuan, B. Zhu, and L. P. Zhu, "Tannin-inspired superhydrophilic and underwater superoleophobic polypropylene membrane for effective oil/water emulsions separation," *Colloids Surfaces A Physicochem. Eng. Asp.*, vol. 522, pp. 585–592, 2017.
- [2] G. A. Gebreslase, "Review on Membranes for the Filtration of Aqueous Based Solution: Oil in Water Emulsion," *J. Membr. Sci. Technol.*, vol. 08, no. 02, pp. 0–16, 2018, doi: 10.4172/2155-9589.1000188.
- [3] E. H. Khader, T. J. Mohammed, and S. W. Adnan, "Reduction of oil and COD from produced water by activated carbon, zeolite, and mixed adsorbents in a fixed-bed column," *Desalin. WATER Treat*, vol. 227, pp. 216–227, 2021.
- [4] H. P. Ngang, A. L. Ahmad, S. C. Low, and B. S. Ooi, "Adsorption-desorption study of oil emulsion towards thermo-responsive PVDF/SiO₂-PNIPAM composite membrane," *J. Environ. Chem. Eng.*, vol. 5, no. 5, pp. 4471–4482, 2017.
- [5] E. H. Khader, T. J. Mohammed, T. M. Albayati, K. T. Rashid, N. M. C. Saady, and S. Zendehboudi, "Green nanoparticles blending with polyacrylonitrile ultrafiltration membrane for antifouling oily wastewater treatment," *Sep. Purif. Technol.*, vol. 353, p. 128256, 2025.
- [6] R. H. Khudhur, N. S. Ali, E. H. Khader, N. S. Abbood, I. K. Salih, and T. M. Albayati, "Adsorption of anionic azo dye from aqueous wastewater using zeolite NaX as an efficient adsorbent," *Desalin. Water Treat.*, vol. 306, pp. 245–252, 2023.
- [7] M. Han, J. Zhang, W. Chu, J. Chen, and G. Zhou, "Research progress and prospects of marine oily wastewater treatment: a review," *Water*, vol. 11, no. 12, p. 2517, 2019.
- [8] T. Ahmad, C. Guria, and A. Mandal, "A review of oily wastewater treatment using ultrafiltration membrane: A parametric study to enhance the membrane performance," *J. Water Process Eng.*, vol. 36, p. 101289, 2020.
- [9] P. Sanghamitra, D. Mazumder, and S. Mukherjee, "Treatment of wastewater containing oil and grease by biological method-a review," *J. Environ. Sci. Heal. Part A*, vol. 56, no. 4, pp. 394–412, 2021.
- [10] M. Padaki, R. S. Murali, M. S. Abdullah, N. Misdan, A. Moslehyani, M. A. Kassim, N. Hilal, and A. F. Ismail, "Membrane technology enhancement in oil–water separation. A review," *Desalination*, vol. 357, pp. 197–207, 2015.
- [11] E. H. Khader, R. H. Khudhur, T. J. Mohammed, O. S. Mahdy, A. A. Sabri, A. S. Mahmood, and T. M. Albayati, "Evaluation of adsorption treatment method for removal of phenol and acetone from industrial wastewater," *Desalin. Water Treat.*, vol. 317, p. 100091, 2024.
- [12] S. Hube, M. Eskafi, K. F. Hrafnkelsdóttir, B. Bjarnadóttir, M. A. Bjarnadóttir, S. Axelsdóttir, and B. Wu, "Direct membrane filtration for wastewater treatment and resource recovery: A review," *Sci. Total Environ.*, vol. 710, p. 136375, 2020.
- [13] E. H. Khader, R. H. Khudhur, N. S. Abbood, and T. M. Albayati, "Decolourisation of anionic azo dye in industrial wastewater using adsorption process: Investigating operating parameters," *Environ. Process.*, vol. 10, no. 2, p. 34, 2023.
- [14] E. Nascimben Santos, Z. László, C. Hodúr, G. Arthanareeswaran, and G. Veréb, "Photocatalytic membrane filtration and its advantages over conventional approaches in the treatment of oily wastewater: A review," *Asia-Pacific J. Chem. Eng.*, vol. 15, no. 5, p. e2533, 2020.
- [15] A. I. Adetunji and A. O. Olaniran, "Treatment of industrial oily wastewater by advanced technologies: a review," *Appl. Water Sci.*, vol. 11, no. 6, pp. 1–19, 2021, doi: 10.1007/s13201-021-01430-4.
- [16] M. Keyvan Hosseini, L. Liu, P. Keyvan Hosseini, A. Bhattacharyya, K. Lee, J. Miao, and B. Chen, "Review of Hollow Fiber (HF) Membrane Filtration Technology for the Treatment of Oily Wastewater: Applications and Challenges," *J. Mar. Sci. Eng.*, vol. 10, no. 9, 2022, doi: 10.3390/jmse10091313.

- [17] E. H. Khader, S. A. Muslim, N. M. C. Saady, N. S. Ali, I. K. Salih, T. J. Mohammed, T. M. Albayati, and S. Zendejboudi, "Recent Advances in Photocatalytic Advanced Oxidation Processes for Organic Compound Degradation: A Review," *Desalin. Water Treat.*, p. 100384, 2024.
- [18] G. Tekin, G. Ersöz, and S. Atalay, "Degradation of benzoic acid by advanced oxidation processes in the presence of Fe or Fe-TiO₂ loaded activated carbon derived from walnut shells: A comparative study," *J. Environ. Chem. Eng.*, vol. 6, no. 2, pp. 1745–1759, 2018.
- [19] S. N. U. S. Bukhari, A. A. Shah, W. Liu, I. A. Channa, A. D. Chandio, I. A. Chandio, and Z. H. Ibupoto, "Activated carbon based TiO₂ nanocomposites (TiO₂@ AC) used simultaneous adsorption and photocatalytic oxidation for the efficient removal of Rhodamine-B (Rh-B)," *Ceram. Int.*, vol. 50, no. 21, pp. 41285–41298, 2024.
- [20] E. Umar, M. Ikram, J. Haider, W. Nabgan, M. Imran, and G. Nazir, "A State-of-Art Review of the Metal Oxide-Based Nanomaterials Effect on Photocatalytic Degradation of Malachite Green Dyes and a Bibliometric Analysis," *Glob. Challenges*, vol. 7, no. 6, pp. 1–18, 2023, doi: 10.1002/gch2.202300001.
- [21] F. Ahmad, S. Nisar, and M. Mehmood, "A Critical Review on the Photo Degradation of Diazinon, A Persistent Organic Pesticides.," *J. Chem. Soc. Pakistan*, vol. 44, no. 5, 2022.
- [22] S. Divya, P. Sivaprakash, S. Raja, S. E. Muthu, I. Kim, N. Renuka, S. Arumugam, and T. H. Oh, "Impact of Zn doping on the dielectric and magnetic properties of CoFe₂O₄ nanoparticles," *Ceram. Int.*, vol. 48, no. 22, pp. 33208–33218, 2022.
- [23] H. Alinezhad, P. H. T. Amiri, S. M. Tavakkoli, R. M. Muhiebes, and Y. F. Mustafa, "Nanoparticles and Their Hybrids as Catalysts," *J. Chem. Rev.*, vol. 4, no. 4, 2022.
- [24] A. Roy, A. Elzaki, V. Tirth, S. Kajoak, H. Osman, A. Algahtani, S. Islam, N. L. Faizo, M. U. Khandaker, M. N. Islam, and T. B. Emran, "Biological synthesis of nanocatalysts and their applications," *Catalysts*, vol. 11, no. 12, p. 1494, 2021.
- [25] A. K. Singh, "A review on plant extract-based route for synthesis of cobalt nanoparticles: Photocatalytic, electrochemical sensing and antibacterial applications," *Curr. Res. Green Sustain. Chem.*, vol. 5, no. January, p. 100270, 2022, doi: 10.1016/j.crgsc.2022.100270.
- [26] P. C. Nagajyothi, S. V. Prabhakar Vattikuti, K. C. Devarayapalli, K. Yoo, J. Shim, and T. V. M. Sreekanth, "Green synthesis: photocatalytic degradation of textile dyes using metal and metal oxide nanoparticles-latest trends and advancements," *Crit. Rev. Environ. Sci. Technol.*, vol. 50, no. 24, pp. 2617–2723, 2020.
- [27] V. Verma, M. Al-Dossari, J. Singh, M. Rawat, M. G. M. Kordy, and M. Shaban, "A review on green synthesis of TiO₂ NPs: photocatalysis and antimicrobial applications," *Polymers (Basel)*, vol. 14, no. 7, p. 1444, 2022.
- [28] H. Li, X. Zhang, Y. Zhang, L. Jia, Y. Zhang, H. Huang, H. Ou, and Y. Zhang, "Adsorbent-to-photocatalyst: Recycling heavy metal cadmium by natural clay mineral for visible-light-driven photocatalytic antibacterial," *J. Colloid Interface Sci.*, vol. 629, pp. 1055–1065, 2023.
- [29] M. Kaur, J. Singh, M. Chauhan, V. Kumar, and K. Singh, "Green synthesis of TiO₂-Al₂O₃-ZnFe₂O₄ nanocomposite using the Hibiscus rosa sinesis and evaluation of its photocatalytic applications," *Open Ceram.*, p. 100571, 2024.
- [30] G. G. Hasan, S. E. Laouini, A. Khelef, H. A. Mohammed, M. Althamthami, S. Meneceur, F. Alharthi, S. A. Alshareef, and F. Mena, "Efficient treatment of oily wastewater, antibacterial activity, and photodegradation of organic dyes using biosynthesized Ag@ Fe₃O₄ nanocomposite," *Bioprocess Biosyst. Eng.*, vol. 47, no. 1, pp. 75–90, 2024.
- [31] L. B. de Menezes, P. C. L. Muraro, D. M. Druzian, Y. P. M. Ruiz, A. Galembeck, G. Pavoski, D. C. R. Espinosa, and W. L. da Silva, "Calcium oxide nanoparticles: Biosynthesis, characterization and photocatalytic activity for application in yellow tartrazine dye removal," *J. Photochem. Photobiol. A Chem.*, vol. 447, p. 115182, 2024.
- [32] N. S. Abbood, N. S. Ali, E. H. Khader, H. S. Majdi, T. M. Albayati, and N. M. C. Saady, "Photocatalytic degradation of cefotaxime pharmaceutical compounds onto a modified nanocatalyst," *Res. Chem. Intermed.*, vol. 49, no. 1, pp. 43–56, 2023.
- [33] V. Vorobyova, M. Skiba, and G. Vasyliov, "Extraction of phenolic compounds from tomato pomace using choline chloride-based deep eutectic solvents," *J. Food Meas. Charact.*, vol. 16, no. 2, pp. 1087–1104, 2022.
- [34] Z. T. Alkanan, A. R. S. Al-Hilphy, A. B. Altemimi, R. Mandal, and A. Pratap-Singh, "Comparison of

- quality characteristics of tomato paste produced under ohmic-vacuum combination heating and conventional heating,” *Appl. Food Res.*, vol. 1, no. 2, p. 100014, 2021, doi: 10.1016/j.afres.2021.100014.
- [35] Y. Gutha, V. S. Munagapati, M. Naushad, and K. Abburi, “Removal of Ni(II) from aqueous solution by *Lycopersicon esculentum* (Tomato) leaf powder as a low-cost biosorbent,” *Desalin. Water Treat.*, vol. 54, no. 1, pp. 200–208, 2015, doi: 10.1080/19443994.2014.880160.
- [36] F. Nadeem, I. A. Bhatti, A. Ashar, M. Yousaf, M. Iqbal, M. Mohsin, J. Nisar, N. Tamam, and N. Alwadai, “Eco-benign biodiesel production from waste cooking oil using eggshell derived MM-CaO catalyst and condition optimization using RSM approach,” *Arab. J. Chem.*, vol. 14, no. 8, p. 103263, 2021.
- [37] X. Zhang, R. Yu, D. Wang, W. Li, and Y. Zhang, “Green Photocatalysis of Organic Pollutants by Bimetallic Zn-Zr Metal-Organic Framework Catalyst,” *Front. Chem.*, vol. 10, no. May, pp. 1–9, 2022, doi: 10.3389/fchem.2022.918941.
- [38] L. M. Alshandoudi, A. Y. Al Subhi, S. A. Al-Isaee, W. A. Shaltout, and A. F. Hassan, “Static adsorption and photocatalytic degradation of amoxicillin using titanium dioxide/hydroxyapatite nanoparticles based on sea scallop shells,” *Environ. Sci. Pollut. Res.*, vol. 30, no. 38, pp. 88704–88723, 2023.
- [39] R. Molinari and P. Argurio, “PMRs in photocatalytic synthesis of organic compounds,” in *Current Trends and Future Developments on (Bio-) Membranes*, Elsevier, 2018, pp. 209–231.
- [40] A. Elhalil, W. Boumya, A. Machrouhi, R. Elmoubarki, S. Mansouri, M. Sadiq, M. Abdennouri, and N. Barka, “Synthesis, characterization and efficient photocatalytic properties of spinel materials for dye degradation,” *Appl. Surf. Sci. Adv.*, vol. 13, no. November 2022, p. 100381, 2023, doi: 10.1016/j.apsadv.2023.100381.
- [41] E. H. Khader, T. J. Mohammed, T. M. Albayati, N. M. C. Saady, and S. Zendejboudi, “Green nanocatalyst for the photocatalytic degradation of organic pollutants in petroleum refinery wastewater: Synthesis, characterization, and optimization,” *J. Mol. Struct.*, vol. 1304, p. 137688, 2024.
- [42] H. A. El-Gawad, E. E. Ebrahiem, M. Y. Ghaly, A. A. Afify, and R. M. Mohamed, “An application of advanced oxidation process on industrial crude oily wastewater treatment,” *Sci. Rep.*, vol. 13, no. 1, p. 3420, 2023.
- [43] K. Sharma, D. Vaya, G. Prasad, and P. K. Surolia, “Photocatalytic process for oily wastewater treatment: A review,” *Int. J. Environ. Sci. Technol.*, vol. 20, no. 4, pp. 4615–4634, 2023.
- [44] M. Mohammadi, S. Sabbaghi, M. Binazadeh, S. Ghaedi, and H. Rajabi, “Type-1 α -Fe₂O₃/TiO₂ photocatalytic degradation of tetracycline from wastewater using CCD-based RSM optimization,” *Chemosphere*, vol. 336, p. 139311, 2023.
- [45] S. P. Santoso, A. E. Angkawijaya, V. Bundjaja, C. W. Hsieh, A. W. Go, M. Yuliana, H. Y. Hsu, P. L. Tran-Nguyen, F. E. Soetaredjo, and S. Ismadji, “TiO₂/guar gum hydrogel composite for adsorption and photodegradation of methylene blue,” *Int. J. Biol. Macromol.*, vol. 193, pp. 721–733, 2021.
- [46] E. H. Khader, N. S. Abbood, T. N. Albyati, and T. J. Mohammed, “Performance evaluation of integral process for treatment of oilfield wastewater,” in *AIP Conference Proceedings*, 2022, vol. 2443, no. 1.
- [47] E. H. Khader, T. J. Mohammed, T.M. Albayati, H. N. Harharah, A. Amari, N. M. C. Saady, and S. Zendejboudi, “Current trends for wastewater treatment technologies with typical configurations of photocatalytic membrane reactor hybrid systems: A review,” *Chem. Eng. Process. - Process Intensif.*, vol. 192, no. May, p. 109503, 2023, doi: 10.1016/j.cep.2023.109503.
- [48] M. Zendejdel, G. Cruciani, and B. Barghi, “Micro-meso structure NaP zeolite @TiO₂ nanocomposite: eco-friendly photocatalyst for simultaneous removal COD and degradation of methylene blue under solar irradiation,” *Photochem. Photobiol. Sci.*, vol. 21, no. 6, pp. 1011–1029, 2022, doi: 10.1007/s43630-022-00190-7.
- [49] H. M. Mehwish, M. S. R. Rajoka, Y. Xiong, H. Cai, R. M. Aadil, Q. Mahmood, Z. He, and Q. Zhu, “Green synthesis of a silver nanoparticle using *Moringa oleifera* seed and its applications for antimicrobial and sun-light mediated photocatalytic water detoxification,” *J. Environ. Chem. Eng.*, vol. 9, no. 4, p. 105290, 2021.
- [50] A. El Golli, S. Contreras, and C. Dridi, “Bio-synthesized ZnO nanoparticles and sunlight-driven photocatalysis for environmentally-friendly and sustainable route of synthetic petroleum refinery wastewater treatment,” *Sci. Rep.*, vol. 13, no. 1, p. 20809, 2023.
- [51] D. A. B. Sidik, N. H. H. Hairom, A. I. Rozman, M. J. S. Johari, and A. Muhammad, “The photocatalytic activity of green zinc oxide nanoparticles in the treatment of aerobically palm oil mill effluent,” *J. Sci.*

Technol., vol. 15, no. 1, pp. 7–15, 2023.

- [52] S. P. Goutam, G. Saxena, V. Singh, A. K. Yadav, R. N. Bharagava, and K. B. Thapa, “Green synthesis of TiO₂ nanoparticles using leaf extract of *Jatropha curcas* L. for photocatalytic degradation of tannery wastewater,” *Chem. Eng. J.*, vol. 336, pp. 386–396, 2018.
- [53] A. El Golli, M. Fendrich, N. Bazzanella, C. Dridi, A. Miotello, and M. Orlandi, “Wastewater remediation with ZnO photocatalysts: green synthesis and solar concentration as an economically and environmentally viable route to application,” *J. Environ. Manage.*, vol. 286, p. 112226, 2021.
- [54] S. Aroob, S. A. Carabineiro, M. B. Taj, I. Bibi, A. Raheel, T. Javed, R. Yahya, W. Alelwani, F. Verpoort, K. Kamwilaisak, and S. Al-Farraj, “Green synthesis and photocatalytic dye degradation activity of CuO nanoparticles,” *Catalysts*, vol. 13, no. 3, p. 502, 2023.
- [55] M. H. Meshkatsadat, M. Zahedifar, and B. Pouramiri, “Facile green synthesis of CaO NPs using the *Crataegus pontica* C. Koch extract for photo-degradation of MB dye,” *Environ. Sci. Pollut. Res.*, vol. 29, no. 36, pp. 54688–54697, 2022.